

ARTICLE OPEN



Matrix protein Tenascin-C promotes kidney fibrosis via STAT3 activation in response to tubular injury

Qionghong Xie^{1,5}, Min Zhang^{1,5}, Xiaoyi Mao^{1,5}, Mingyue Xu¹, Shaojun Liu¹, Da Shang¹, Yunyu Xu¹, Ruiying Chen¹, Yi Guan¹, Xinzhong Huang², Roy Zent^{3,4}, Ambra Pozzi^{3,4} and Chuan-Ming Hao¹✉

© The Author(s) 2022

Accumulating evidence indicates that the extracellular matrix (ECM) is not only a consequence of fibrosis, but also contributes to the progression of fibrosis, by creating a profibrotic microenvironment. Tenascin-C (TNC) is an ECM glycoprotein that contains multiple functional domains. We showed that following kidney injury, TNC was markedly induced in fibrotic areas in the kidney from both mouse models and humans with kidney diseases. Genetically deletion of TNC in mice significantly attenuated unilateral ureteral obstruction-induced kidney fibrosis. Further studies showed that TNC promoted the proliferation of kidney interstitial cells via STAT3 activation. TNC-expressing cells in fibrotic kidney were activated fibroblast 2 (Act.Fib2) subpopulation, according to a previously generated single nucleus RNA-seq dataset profiling kidney of mouse UO model at day 14. To identify and characterize TNC-expressing cells, we generated a TNC-promoter-driven CreER2-IRES-eGFP knock-in mouse line and found that the TNC reporter eGFP was markedly induced in cells around injured tubules that had lost epithelial markers, suggesting TNC was induced in response to epithelium injury. Most of the eGFP-positive cells were both NG2 and PDGFR β positive. These cells did not carry markers of progenitor cells or macrophages. In conclusion, this study provides strong evidence that matrix protein TNC contributes to kidney fibrosis. TNC pathway may serve as a potential therapeutic target for interstitial fibrosis and the progression of chronic kidney disease.

Cell Death and Disease (2022)13:1044; <https://doi.org/10.1038/s41419-022-05496-z>

BACKGROUND

Kidney fibrosis is the final common pathway to end-stage renal disease and characterized by extracellular matrix (ECM) accumulation and destruction of normal structure [1, 2]. Accumulating evidence indicates that the ECM is not only a consequence of fibrosis, but also contributes to the progression of fibrosis, by creating a profibrotic microenvironment or a fibrogenic niche [3, 4].

It has been documented that the ECM not only provides physical scaffolds to cells by forming a three-dimensional network, but also regulates many biologic processes including proliferation, migration, differentiation, survival and morphogenesis during development or in certain physiological/pathophysiological conditions [5–7]. Matricellular proteins (or non-structural matrix proteins) are a group of ECM proteins that are characterized by dynamical expressions and regulatory roles [8]. Rather than serving as stable structural elements, they are usually transiently expressed during development or after injury [9]. They contain multiple functional domains, such as binding sites for other ECM proteins, ligands for cell surface receptors, and sites that can sequester specific growth factors, playing important roles in regulating cellular processes [10].

Tenascin-C (TNC), a hexameric glycoprotein, is a member of the matricellular proteins that is expressed during development and is at low levels in most of the adult tissues, but re-induced following injury and associated with the severity of diseases and prognosis [11, 12]. The monomer of TNC contains an N-terminal assembly domain, epidermal growth factor-like (EGF-L) repeats, fibronectin type-III (FNIII) like repeats and a C-terminal fibrinogen-like globe [13, 14]. These functional domains have been suggested to interact with specific cell-surface receptors, such as epidermal growth factor receptor (EGFR), integrins and toll-like receptor 4 (TLR4) [13]. They can also recruit cytokines and growth factors, and present them to or prevent them from cell-surface receptors depending on their relative locations [14]. Mice lacking TNC develop normally, suggesting that TNC is not indispensable for development. However, accumulating evidence show that TNC is markedly increased in the fibrotic tissues and associated with organ fibrosis [15–17]. Recently, TNC was also found to promote renal interstitial fibroblast proliferation via integrin/focal adhesion kinase/mitogen-activated protein kinase pathway [18].

In the present study, we characterized the cells that expressed TNC and examined their role in renal fibrosis. This study provided novel information about the role of TNC in renal fibrosis.

¹Division of Nephrology, Huashan Hospital, Fudan University, Shanghai, China. ²Division of Nephrology, Affiliated Hospital of Nantong University, Nantong, China. ³Division of Nephrology, Vanderbilt University Medical Center, Nashville, TN, USA. ⁴Department of Veterans Affairs, Nashville, TN, USA. ⁵These authors contributed equally: Qionghong Xie, Min Zhang, Xiaoyi Mao. ✉email: chuanminghao@fudan.edu.cn
Edited by Professor Hans-Uwe Simon

Received: 26 August 2022 Revised: 29 November 2022 Accepted: 5 December 2022

Published online: 15 December 2022

METHODS

Patients

To characterize the distribution of TNC expression in normal human kidney, specimens from healthy parts of human carcinoma nephrectomy were obtained. TNC mRNA was measured by qPCR in fresh tissue, and the distribution of TNC protein was investigated in paraffin-embedded tissue by immunohistochemistry (IHC). To examine the induction of TNC in diseased kidneys, TNC protein was detected in paraffin-embedded sections from patients with biopsy-proven interstitial fibrosis (IgA nephropathy) by IHC. This study was approved by the ethics committee of Huashan Hospital, Fudan University, and informed consents were signed.

Animals and Models

Mice. TNC^{CreER2-eGFP/+} mouse line was generated as described previously [19]. In brief, an inducible CreER2 gene with an eGFP reporter was knocked into the 2nd exon of TNC at the site of starting codon ATG. The insertion of this cassette also resulted in TNC deletion (Fig. 2A). The TNC deletion (TNC^{-/-}) mice were fertile, and developed normally. Male TNC^{-/-} mice and their wild-type littermates, aged 8–12 weeks, were used to examine the role of TNC in fibrosis. R26^{tdTomato} reporter mice were purchased from the Jackson Laboratory (stock number, 007909). The bi-transgenic TNC^{CreER2-eGFP/+};R26^{tdTomato/+} reporter mice were generated by crossing TNC^{CreER2-eGFP/+} with R26^{tdTomato} mice. All of the mice were maintained in the animal facility of Fudan University and allowed free access to standard rodent chow and water. All of the animal experiments were approved by the Institutional Animal Care and Use Committees of Fudan University.

TNC reporter mice. In the TNC^{CreER2-eGFP/+} mice, eGFP is driven by endogenous TNC promoter (TNCp-CreER2-IRES-eGFP), and is thus used as a TNC reporter. In the bi-transgenic TNC^{CreER2-eGFP/+};R26^{tdTomato/+} reporter mice, the recombination is induced by TNC-promoter-driven CreER2 in the presence of tamoxifen, and then tdTomato (red fluorescence protein) will label the TNC-expressing cells and their daughter cells permanently.

Models. UUO-induced kidney fibrosis model was used in our study. The mice were anesthetized with chloral hydrate (400 mg/kg body weight) by intra-peritoneal injection and body temperatures were maintained at 36.5–37.5 °C throughout the procedure. The left ureter was exposed via a flank incision and ligated with two 3.0 silk ties at the level of the lower renal pole. The mice were sacrificed at day 7, 10, or 14 after the operation. The EdU (Invitrogen, C10339) cooperation assay was used to assess cell proliferation of the kidney: 0.1 mg of EdU was injected (i.p.) at day 3 and 5 after UUO operation and the mice were sacrificed at day 7. Each group for comparison included 6 to 8 mice. The investigators were blinded to the animal when accessing the outcomes.

Cell experiments

Cell lines. The TNC-expressing cells (TNC-Cell) were obtained by sorting the tdTomato-positive cells in the UUO kidneys of TNC^{CreER2-eGFP/+};R26^{tdTomato/+} mice using flow cytometry, and immortalized using SV40 T lentivirus (Fig. 9B). This cell line was cultured in polylysine (20 µg/mL, Sigma, P1399) coated dish with DMEM/F12 media containing 10% FBS, 1 ng/mL basic-FGF (Peprotech, 400-29) and 5 ng/mL insulin (Sigma, I0305000). The normal rat kidney fibroblast NRK49F was purchased from American Type Culture Collection (ATCC). Both NRK49F and mouse embryo fibroblast NIH3T3 were cultured in DMEM media (GIBCO, C11995500BT) containing 10% heat-inactivated fetal bovine serum (FBS, GIBCO, 10270-106), 100U/ml penicillin and 100 µg/ml streptomycin. Mycoplasma contamination was tested by polymerase chain reaction (PCR). Cells were incubated at 37 °C in a 5% CO₂, humidified atmosphere.

Intervention. The cultured cells at 60% confluence were incubated with 1% FBS-containing media for 24 h followed by treatment of human TNC (Millipore, CC605, 5 µg/mL or 10 µg/mL) or TGFβ (2 ng/mL to 10 ng/mL, Sigma, APREST95171). The STAT3 inhibitor Stattic (Selleck, S7024, 2 µM) or EGFR inhibitor Gefitinib (5 µM, Selleck, ZD-1839) were added to the media 30 min before TNC treatment.

Cell Proliferation. After TNC treatment for 24 h, the number and viability of the cultured cells were determined using the Cell Counting Kit-8 (CCK-8, Dojindo Laboratories, CK04) following the manufacturer's instructions. Briefly, water-soluble tetrazolium salt WST-8 is reduced by dehydrogenase in the cells and turns into an orange formazan dye which is soluble in the

culture media, and the amount of the formazan dye is proportional to the number of living cells. The cell proliferation was determined by detecting the proportion of EdU-positive cells using the Click-iT® EdU Imaging Kits (Invitrogen, C10339) according to the manufacturer's instructions. EdU is detected based on a copper-catalyzed covalent reaction between an alkyne (contained in the EdU) and azide (contained in the Alexa Fluor dye).

Histology and pathology

Tissue preparation. The mice were anesthetized with chloral hydrate (500 mg/kg body weight) intra-peritoneal injection before sacrifice and immediately perfused with 60 ml ice-cold PBS via the left ventricle. The kidneys were hemi-sectioned horizontally and fixed in 4% paraformaldehyde (PFA) on ice for 1 hp. Then half of each kidney was incubated in 30% sucrose-PBS at 4 °C overnight and embedded in OCT, and the other half was processed and embedded in paraffin.

Immunohistochemistry. Paraffin-embedded 2 µm-thick sections of the human kidney were deparaffinized and rehydrated in water. After incubation with 3% H₂O₂ for 30 min at room temperature (RT), the tissues were given microwave antigen retrieval in citrate buffer pH 6.0 (100% power for 10 min), blocked with 5% BSA in PBS for 1 h at RT, and followed by the incubation with anti-human TNC antibody (Sigma rabbit polyclonal, HPA004823, 1:500) at 4 °C overnight. After 3 washes with PBS, the samples were incubated in horseradish peroxidase (HRP) conjugated secondary antibody for 45 min at RT, followed by coloration with 3,3'-diaminobenzidine solution (DAB, Gene Tech, GK6005).

Immunofluorescence. Frozen tissue embedded in OCT was cut into 5 µm thick section. For IF analysis, the sections were fixed in cold acetone for 3 min, washed in PBS, blocked in 5% bovine serum albumin (BSA) for 30 min and then incubated with primary antibodies in blocking buffer overnight at 4 °C. The primary antibodies included: anti-GFP (Abcam rabbit polyclonal, ab290, 1:200; Aves Labs chicken antibodies, GFP-1020, 1:500), anti-AQP2 (Santa Cruz goat polyclonal, sc-9882, 1:100), anti-CD31 (Abcam rat monoclonal, ab56299, 1:100), anti-PDGFRβ (eBioscience rat monoclonal, 14-1402, 1:100), anti-CD34 (Abcam rat monoclonal, ab8158, 1:200), anti-CD44 (Abcam rat monoclonal, ab119863, 1:200), anti-α-SMA (Sigma mouse monoclonal, C6198, 1:100), anti-FSP-1 (Abcam rabbit polyclonal, ab27957, 1:200), anti-NG2 (Millipore rabbit polyclonal, AB5320B, 1:100), anti-TNC (Sigma rat monoclonal, T2551, 1:100), anti-F4/80 (AbD serotec rat monoclonal, MAC497R, 1:200), anti-CD68 (AbD serotec rat monoclonal, MAC497R, 1:200), and anti-THP (Santa Cruz rabbit polyclonal, sc-20631, 1:200) antibody. After 3 washes in PBS, the tissue was incubated with FITC- or Cy3- conjugated anti-IgG/IgY secondary antibody (Millipore, 1:200) for 1 h at room temperature (RT), followed by 3 washes in PBS and then covered by Vectashield Mounting Medium with DAPI (Vector Labs, H-1200-10). Fluorescein lotus tetragonolobus lectin (LTL, Vector Labs, FL-1321-2, 1:100) was used to label proximal tubules.

EdU detection. Paraffin-embedded renal tissue from the mice which had received EdU (Invitrogen, C10339) injection after the operation was used for EdU detection according to the manufacturer's instructions. EdU-positive cells were calculated per high power field to compare the proliferation between wild type and TNC^{-/-} mice.

Quantitative RT-PCRs

Renal cortex and papilla isolated from mice kidneys were used to measure TNC mRNA and TNC reporter eGFP mRNA to determine the expression of TNC in different regions of kidney. The entire kidney from UUO model was homogenized to exam the TNC expression and evaluate the severity of fibrosis by detecting the mRNA of TNC, collagen Ia, fibronectin and PAI-1. Total mRNA was extracted using TRIzol Reagent (Invitrogen), reversely transcribed using RevertAid RT reagent Kit (Takara) according to the manufacturer's protocol. Levels of mRNA were determined by real time qPCR using SYBR Premix Ex Taq (Takara) and normalized to the eukaryotic 18 s rRNA or β-actin. The primers used were TNC: F 5'-CAA CTG TGC CCT GTC CTA C-3', R 5'-AAC GCC CTG ACT GTG GTT A-3'; eGFP: F 5'-CCT CAA GGA CGA CGG CAA C-3', R 5'-CTC GAT GCG GTT CAC CAG-3'; collagen Ia: F 5'-TGA CTG GAA GAG CGG AGA G-3', R 5'-GAC GGC TGA GTA GGG AAC A-3'; fibronectin: F 5'-TGG GAG CAT TGT TGT GTC-3', R 5'-AGC GGT GTC ACT ACT CTG T-3'; PAI-1: F 5'-ACT TTA CCC CTC CGA GAA-3', R 5'-CCT GCT GAA ACA CTT TTA C-3'.

Western Blot

Total protein was extracted from the whole kidney or cultured cells using RIPA buffer (0.05 M Tris, 0.15 M NaCl, 1% Triton X-100, 1% sodium deoxycholate, 0.1% SDS, pH7.4) with PMSF, protease inhibitor cocktail and phosphatase inhibitor cocktail (Roche). The concentration of the protein was determined using the BCA protein assay kit (Beyotime). For Western blot, equal amount of protein (20–50 µg per lane) was loaded in a 7.5% or 10% SDS-PAGE mini-gel and transferred to a PVDF membrane (Millipore). The membrane was blocked with 5% BSA in PBST buffer (100 mM PBS, pH 7.5, 0.1% Tween-20) and then incubated in primary antibody diluted with blocking buffer overnight at 4 °C. The primary antibodies included: anti-TNC (IBL, 10337), anti-collagen Ia (Novus, NBP1-30054), anti-αSMA (Sigma, A2066), anti-STAT3 (CST, 12640), anti-phospho-STAT3 (Tyr 705, Abcam, ab76315), anti-EGFR (abcam, ab52894), anti-phospho-EGFR (TYR1068, CST, 2234), anti-GAPDH (CST, 5174) and anti-β-actin (Proteintech, 66009-1-Ig) antibody. Membranes were then incubated with appropriate secondary antibodies and subjected to chemiluminescence detection using ECL Reagent (Millipore, WBKLS0500).

Single Nucleus RNA Sequencing Analysis

UOU day 14 single-cell dataset was downloaded from GEO (GSE119531) [20]. The dataset was processed and analyzed using Seurat software [21]. Data was normalized using “LogNormalize” with a scale factor of 10000. The top 2000 most variable genes were identified using “vst” method. The atlas was subjected to scaling using all genes and PCA analysis using the top 2000 most variable genes. The UMAP embedding was obtained using the top 30 principal components. The cells were annotated the same as reported by the original study. To improve visualization, the cellular identity was sorted as following: JGA, Pod, PT(S1), PT(S2), PT(S3), Prolif. PT, Dediff. PT, DL and tAL, TAL, CNT, DCT, CD-PC, IC, EC, Act. Fib1, Act. Fib2, MP.

Statistical analysis

Statistical analysis was performed using Prism 9.0 (GraphPad Software Inc.). Comparison of two factors was performed by two-tailed *t* test and comparison of two factors with multiple levels was performed by two-way ANOVA test. A *P* value < 0.05 was considered significant. The results were presented as means and error bars indicate ±SEM.

RESULTS

TNC was constitutively expressed by the renal medullary stromal cells in normal kidney

To determine the distribution of TNC in non-fibrosis kidneys, we examined TNC expression using immunohistochemistry (IHC) in non-fibrosis human kidneys and found that TNC immuno-protein was primarily located in the interstitium of renal medulla, but rarely detected in the renal cortex (Fig. 1A, B). This result was supported by TNC mRNA measurement in human kidneys which were resected because of renal carcinoma (Fig. 1C).

Since TNC is an extracellular matrix protein, IHC will not be able to identify cells that express TNC. Therefore, we developed a TNC-promoter-driven eGFP reporter mice (Fig. 1D) [19]. TNC and eGFP mRNA measurement in wild-type or eGFP reporter mouse kidneys also supported that TNC was predominantly expressed in renal papilla (Fig. 1E). Co-staining for TNC reporter eGFP and AQP2, a marker of collecting ducts, showed that eGFP positive cells were not epithelial cells. They were primarily expressed by the renal medullary interstitial cells (RMICs) in normal mouse kidney (Fig. 1F, G and Supplementary 1F, G) [22, 23]. To characterize the cell types that expressed TNC, we co-stained eGFP with specific cell markers in normal kidney and found that eGFP-positive cells expressed platelet-derived growth factor receptor beta (PDGFRβ), a marker of stromal cells of mesenchymal origin [24] (Fig. 1H and Supplement 1H). They did not express CD31 (a marker of endothelial cells [25]), CD34 (a marker of endothelial cells and early hematopoietic stem cells and progenitors [26]), or CD44 (a marker of progenitors [27, 28]), suggesting that TNC was neither expressed in endothelial cells nor progenitor cells (Fig. 1I–K and Supplementary 1I–K). In the normal renal medulla, there were only a few cells positive for αSMA (a marker of myofibroblasts [29]),

FSP1 (recognized as a specific marker of fibroblasts [30], but subsequently identified as a marker of macrophages [31]), or NG2 (a transmembrane glycoprotein used to label pericytes [32]). We did not find eGFP was colocalized with these three markers (Fig. 1L–N and Supplementary Fig. 1L–N).

TNC was markedly induced in the fibrotic area of diseased kidney

We previously reported that TNC was significantly increased in injured glomeruli of IgA nephropathy and expressed by PDGFRβ positive mesangial cells [33]. TNC was also markedly induced in the fibrotic interstitial area of the renal cortex of biopsy specimens from patients with IgA nephropathy or from patients with diabetic nephropathy (Fig. 2A). To further examine the expression of TNC in kidney fibrosis, we generated a unilateral ureteral obstruction (UOU) mouse model and found that TNC protein and mRNA were significantly increased in the fibrotic kidneys (Fig. 2B, C, E). Transgenic TNC reporter mice also showed a remarkable increase of eGFP mRNA expression and eGFP positive cells in the UOU kidneys (Fig. 2D, F). Similar results were also found in the ischemia reperfusion (IR) induced kidney fibrosis model (Supplementary Fig. 2).

TNC deficiency reduced kidney fibrosis in animal models

To investigate the role of TNC induction in kidney fibrosis, we generated a TNC homozygous knockout mice. Deletion of TNC (TNC^{-/-}) significantly attenuated the induction of collagen I expression in the kidneys assessed by IF following UOU by approximate 30% at day 7 and 10 compared with their wild-type littermates (Fig. 3A, *p* < 0.05). Consistently, mRNAs of fibrosis markers, such as collagen Ia, fibronectin and plasminogen activator inhibitor-1 (PAI-1), were significantly lower in the TNC^{-/-} mice after UOU at day 7 and 10 (Fig. 3B, *p* < 0.05). Western blot showed that the proteins of collagen Ia and αSMA were also significantly reduced in TNC^{-/-} mice after UOU at day 7 (Fig. 3C, *n* = 7, *p* < 0.05).

TNC enhanced fibrosis by promoting fibroblasts proliferation via STAT3 pathway

To explore the mechanism by which TNC enhanced fibrosis, we examined the effect of TNC on interstitial cell proliferation and the potential signaling mechanism. Firstly, we evaluated the cell proliferation using EdU incorporation study. In vivo, EdU-positive cells were markedly increased and predominantly located in the renal interstitium after UOU, and TNC deletion significantly reduced the number of EdU-positive cells in the obstructed kidney compared with wild-type mouse (Fig. 4A). To further examine the effect of TNC on cell proliferation, we cultured TNC-Cell (an interstitial cell line obtained from fibrotic kidney, Fig. 4B), NIH3T3 and NRK49F cells. Exogenous TNC dose-dependently increased the number of these cultured cells as assessed by CCK8 kit (Fig. 4C–E). Exogenous TNC also markedly increased EdU incorporation in NRK49F cells, consistent with increasing cell proliferation (Fig. 4F).

To determine the signaling mechanism by which TNC-promoted cell proliferation, we screened 45 phospho-kinases in cultured fibroblast treated with or without TNC, and identified STAT3 as one of the candidates that responded to TNC treatment. The potential significance of STAT3 signaling in mediating the effect of TNC was further validated in UOU kidney and cultured cells. In vivo, the STAT3 and phospho-STAT3 levels were markedly increased after UOU, and TNC deletion significantly reduced the phospho-STAT3 levels (Fig. 5A). In cultured cells fibroblasts, TNC markedly increased the phosphorylation of STAT3, peaking at 45 min (Fig. 5B, C). The effect of TNC on cell proliferation was blocked by the STAT3 inhibitor Stattic (Fig. 5D). It has been well documented that STAT3 is a downstream target of the epidermal growth factor receptor (EGFR). TNC also increased the phosphorylation of EGFR (Fig. 5E), and inhibitor of EGFR reduced the cell number of TNC-induced fibroblasts proliferation (Fig. 5F).

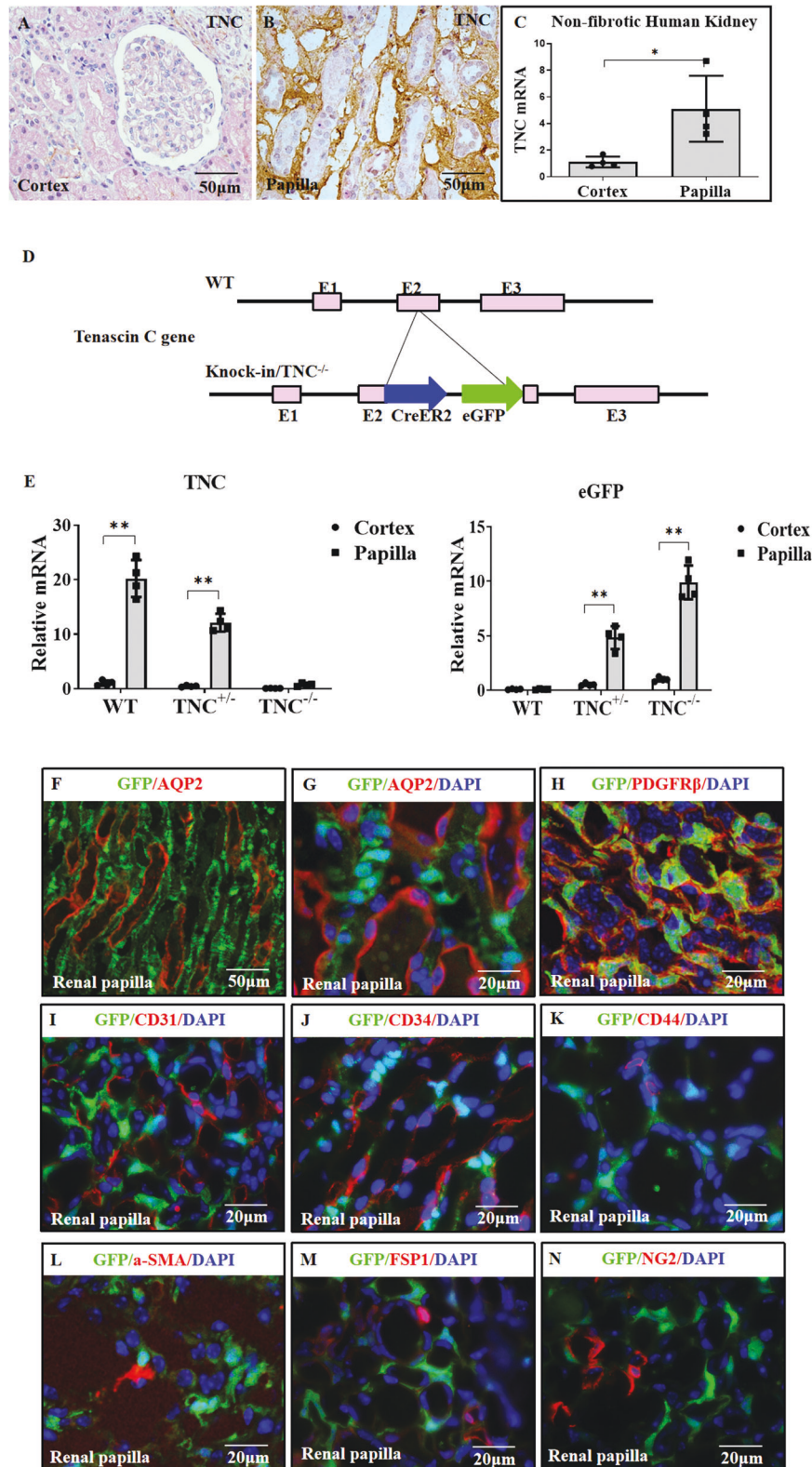


Fig. 1 TNC was constitutively expressed by renal medullary stromal cells in normal kidney. In normal human kidney (kidneys resected because of renal carcinoma), TNC was rarely detected in the cortex, but rich in the medullary interstitium (A, B, $n = 4$, 4 sections for each). Quantitative PCR also showed TNC mRNA was significantly higher in non-fibrotic renal papilla than in cortex (C, $n = 4$, $p = 0.019$). To explore the role of TNC, a TNC-promoter-driven inducible CreER2 knock-in mouse line with an eGFP reporter was generated, and the insertion of CreER2-eGFP lead to TNC deletion (D). Messenger RNA of TNC and TNC reporter eGFP was significantly higher in the renal papilla than in the renal cortex (E, $n = 4$ for each, $p < 0.01$). Co-staining for eGFP and AQP2 showed that eGFP-positive cells were located in the renal medullary interstitium (F, G). These eGFP-positive cells were PDGFR β positive, consistent with stromal cells (H), but negative for CD31 (a marker of endothelial cells, I), CD34 (a marker of endothelial cells and early hematopoietic stem cells and progenitors, J) and CD44 (a marker of progenitors, K). They were also negative for α SMA (a marker of myofibroblasts, L), FSP1 (a marker of fibroblasts, M) and NG2 (a marker of pericytes, N). ($n = 4$, 3 slides for each).

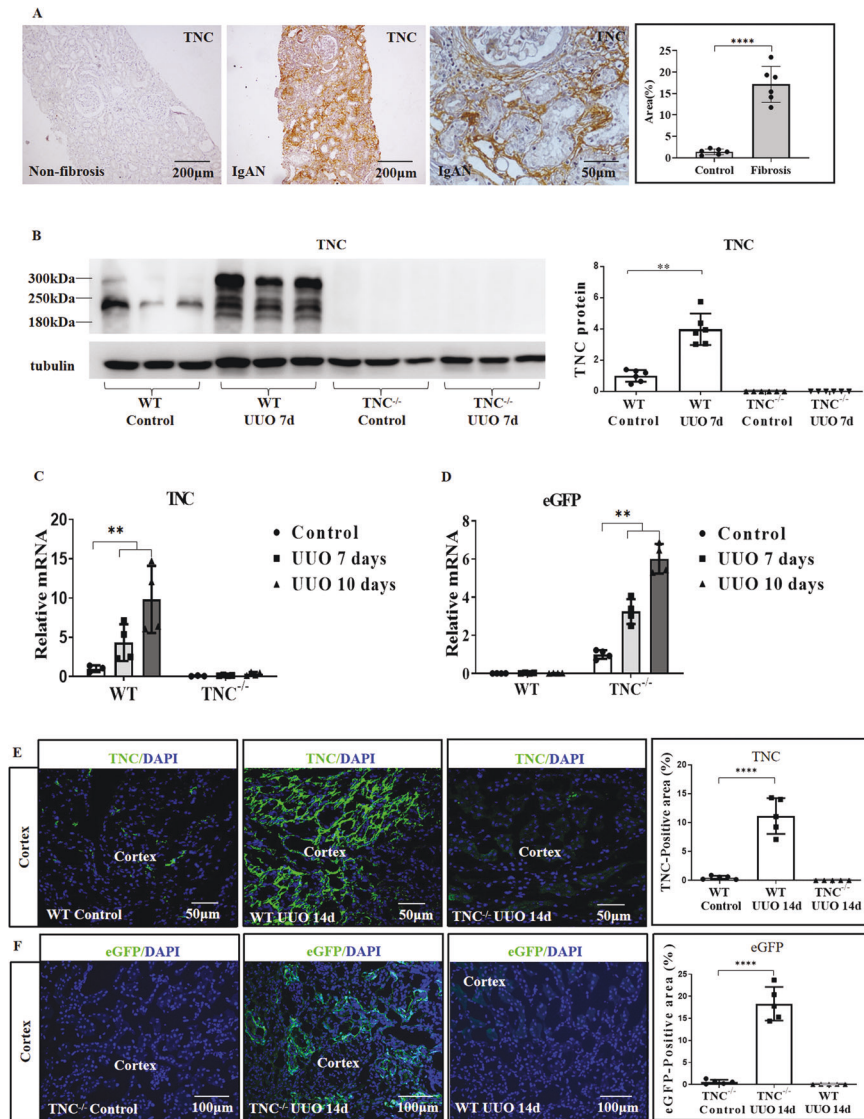


Fig. 2 TNC was significantly increased in the fibrotic kidneys. In patients, TNC level was low in renal cortex of non-fibrotic kidney with minimal change disease, and significantly increased in fibrotic kidneys with IgA nephropathy (A, $n = 6$, $p < 0.0001$). In UUO induced kidney fibrosis mouse model, TNC protein was dramatically increased with different splicing variants (B, $n = 6$, $p < 0.01$), and TNC mRNA in wild-type mice and eGFP mRNA in eGFP reporter mice were also significantly elevated (C, D, $n = 4$ for each time point $p < 0.01$). IF showed that TNC was markedly increased in renal cortex, and eGFP staining in the reporter mice confirmed this result (E, F, $n = 5$, $p < 0.0001$).

TNC-expressing cells in fibrotic kidneys surrounded the injured tubules

To confirm the above results that TNC-expressing cells were significantly induced in fibrosis and explore their characterization, we generated another TNC mouse reporter $TNC^{CreER2-eGFP/+}; R26^{tdTomato/+}$, in which the cells that express TNC will be labeled with red fluorescence protein tdTomato permanently following tamoxifen (Fig. 6A). There are some differences between tdTomato reporter mice and eGFP reporter mice. First, the tdTomato reporter not only labels the cells which are expressing TNC but also the cells once expressed TNC, while the eGFP reporter only labels the cells which are expressing TNC. Second, tdTomato is only expressed in the presence of tamoxifen while eGFP not. Third, the expression of tdTomato is driven by the promoter *Rosa26* and the expression level is high with strong autofluorescence. The tdTomato expression does not reflect TNC expression, while eGFP does. Fourth, the downstream IRES-eGFP protein may be less efficiently translated than the coding sequence of Cre which is directly adjacent to the promoter. However, tamoxifen induction efficiency as well as excision rate vary among tissue types.

Using this bi-transgenic reporter mice $TNC^{CreER2-eGFP/+}; R26^{tdTomato/+}$, we confirmed that TNC-expressing cells were primarily expressed in the medulla of normal kidney (Fig. 6B, E). Then we generated UUO model in this mice and administered tamoxifen right after operation, and found that the tdTomato positive cells were significantly increased in the cortex of fibrotic kidneys (Fig. 6C, D, F). These tdTomato-positive cells were neither stained for Lotus tetragonolobus lectin (LTL, proximal tubule) nor expressed AQP2 (collecting duct), suggesting that they were not epithelial cells (Fig. 6G, H and Supplementary Fig. 3).

Interestingly, these tdTomato positive cells and the other TNC reporter eGFP positive cells in the UUO model were predominantly located adjacent to the tubular structures that were dilated and negative for LTL, THP (Tamm-Horsfall protein, a marker of the thick ascending limb), AQP2, and CD31 (Fig. 7A–C and Supplementary Fig. 4). To examine whether these tubular structures surrounded by TNC reporter positive cells were injured renal tubules, we co-labeled TNC reporter with LTL or antibodies against THP or AQP2 on serial sections. This serial section study showed

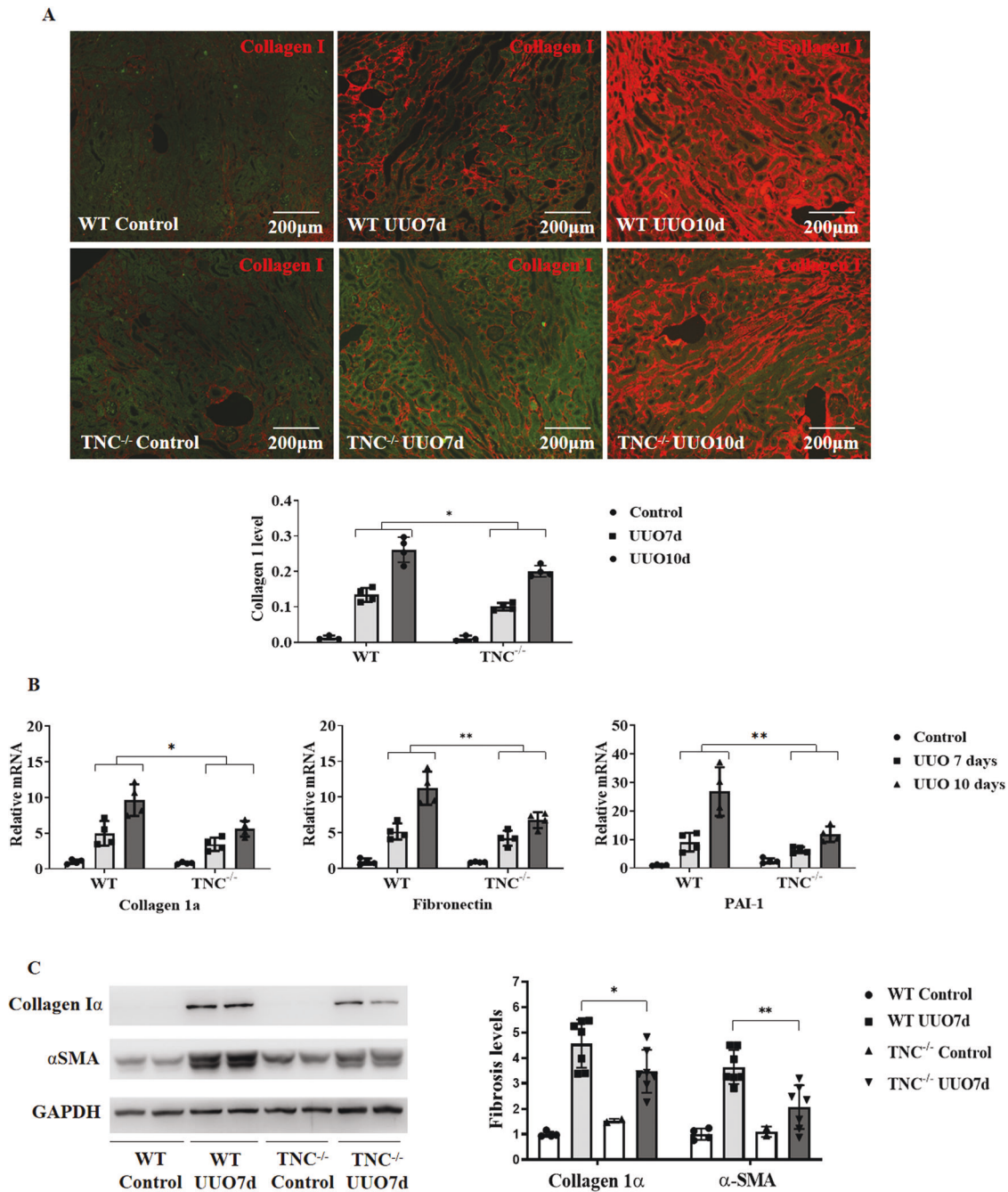


Fig. 3 TNC deficiency reduced kidney fibrosis in animal models. Deletion of TNC ($TNC^{-/-}$) significantly attenuated the induction of collagen I assessed by IF following UO by approximately 30% at day 7 and 10 compared with their wild-type littermates (**A**, $n = 4$ for each time point, two-way ANOVA $p < 0.05$). Consistently, the expression of fibrosis markers, such as collagen 1α , fibronectin and plasminogen activator inhibitor-1 (PAI-1), were significantly lower in $TNC^{-/-}$ mice at UO day 7 and 10 (**B**, $n = 4$ for each time point, two-way ANOVA, $p < 0.05$). Western blot showed that the proteins of collagen 1α and α -SMA were also significantly reduced in $TNC^{-/-}$ mice at UO day 7 (**C**, $n = 7$, $p < 0.05$).

that the tubules surrounded by TNC-expressing cells had continuation to the tubules with positive AQP2 staining, supporting that TNC-expressing cells were localized surrounding the injured tubular epithelial cells in UO kidneys (Fig. 7C and Supplementary Fig. 4C).

TNC-expressing cells in fibrotic kidneys were mostly PDGFR β ⁺NG2⁺ fibroblasts

To investigate TNC expression in the fibrotic kidneys, we used a previously generated single nucleus RNA-seq dataset profiling

kidney of mouse UO model at day 14 (Supplementary Fig. 5A–C). Two subpopulations of activated fibroblasts were identified, with distinct TNC-expression pattern. Around 60% of activated fibroblast 2 (Act.Fib2) expressed TNC, while less than 5% of activated fibroblast 1 expressed TNC. Six percent of the activated fibroblast 2 expressed PDGFR β , NG2 and CD44. Fibroblasts were almost completely negative for FSP1, CD34, F4/80 and CD68 (Fig. 8).

To characterize the cells that express TNC in the fibrotic kidneys, we co-labeled TNC reporter eGFP with specific markers in UO

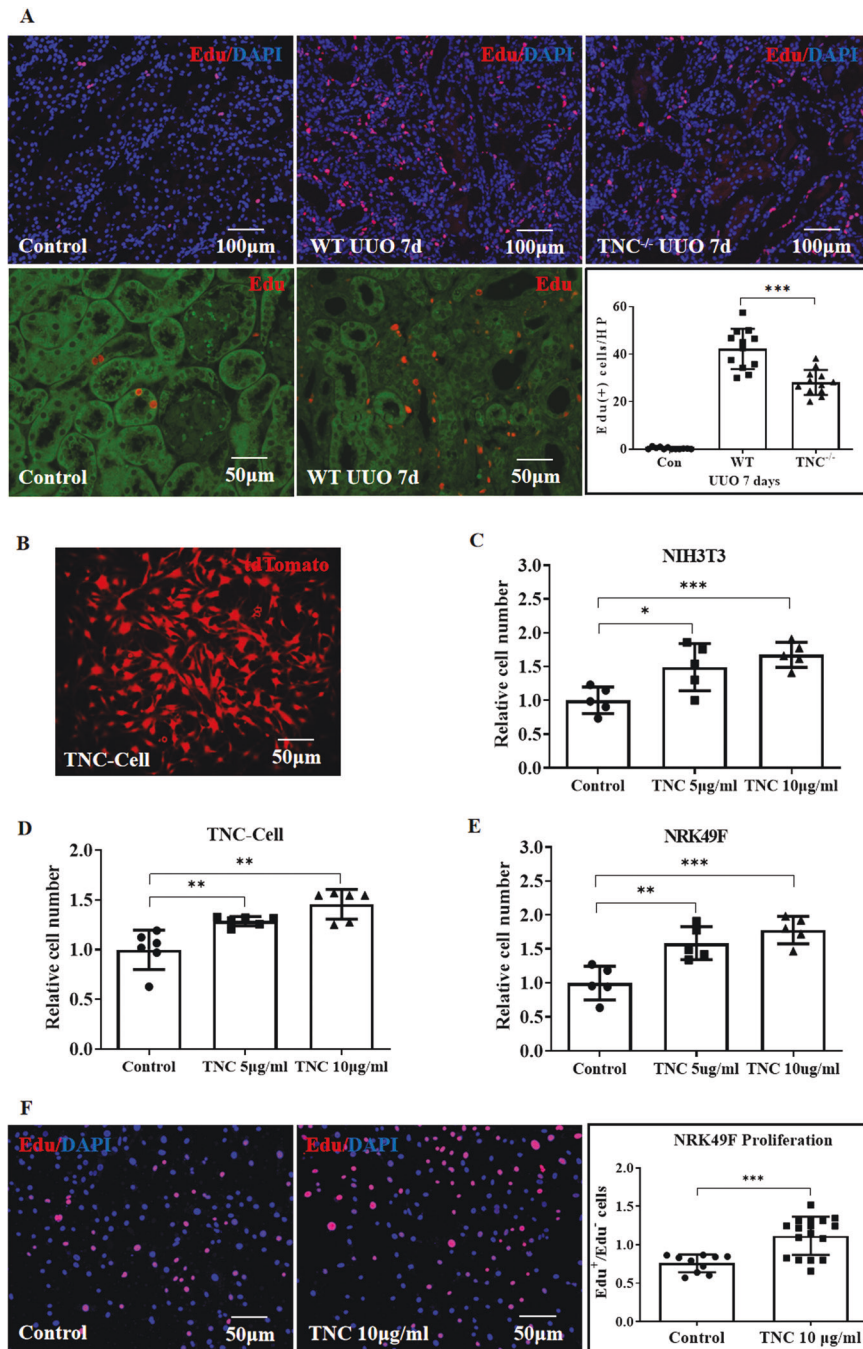


Fig. 4 TNC promoted fibroblasts proliferation. In vivo, EdU positive cells were markedly increased and predominantly located in the renal interstitium after UO, and TNC deletion significantly reduced the number of EdU-positive cells in the obstructed kidney compared with wild-type mouse (A, $n = 4$ mice, 3 slides for each mouse, $p < 0.05$). To further examine the effect of TNC on cell proliferation, TNC-expressing cells (TNC-Cell) were obtained by sorting the tdTomato-positive cells in UO kidneys, and then immortalized by transfecting SV40 T lentivirus (B). Exogenous TNC dose dependently increased the cell number of TNC-Cell, NIH3T3 and NRK49F in vitro, assessed by CCK8 kit (C–E, $p < 0.01$). Exogenous TNC also markedly increased EdU incorporation in NRK49F cells, consistent with promoting cell proliferation (F, $p < 0.001$).

model. We did not use tdTomato as reporter because its autofluorescence is too strong that it can be detected in the green channel. We found that the eGFP-positive cells were positive for PDGFR β , consistent with stromal cells (Fig. 9A and Supplementary Fig. 6A). Most of eGFP-positive cells were NG2 (a marker of pericyte) positive (Fig. 9B, I and Supplement Fig. 6B). Some of the eGFP-positive cells were α SMA positive, while most of α SMA positive myofibroblasts were not eGFP positive (Fig. 9C, J and Supplement Fig. 6C). None of the eGFP positive cells were positive for FSP1 (Fig. 9D and Supplementary Fig. 6D). In addition,

the eGFP positive cells were neither CD34 nor CD44 positive (Fig. 9E, F and Supplementary Fig. 6E, F), and were neither CD68 nor F4/80 (markers of macrophages) positive (Fig. 9G, H and Supplementary Fig. 6G, H).

In addition, it has been reported that renal papilla contains stem cells [34], and TNC has also been reported to be expressed in stem cells [35]. To determine whether the TNC-expressing cells in normal renal medulla were progenitors or source of the expanded stromal cells in the renal cortex after fibrosis, we conducted a cell lineage tracing study in TNC^{CreER2-eGFP/+};R26^{tdTomato/+} mice. We

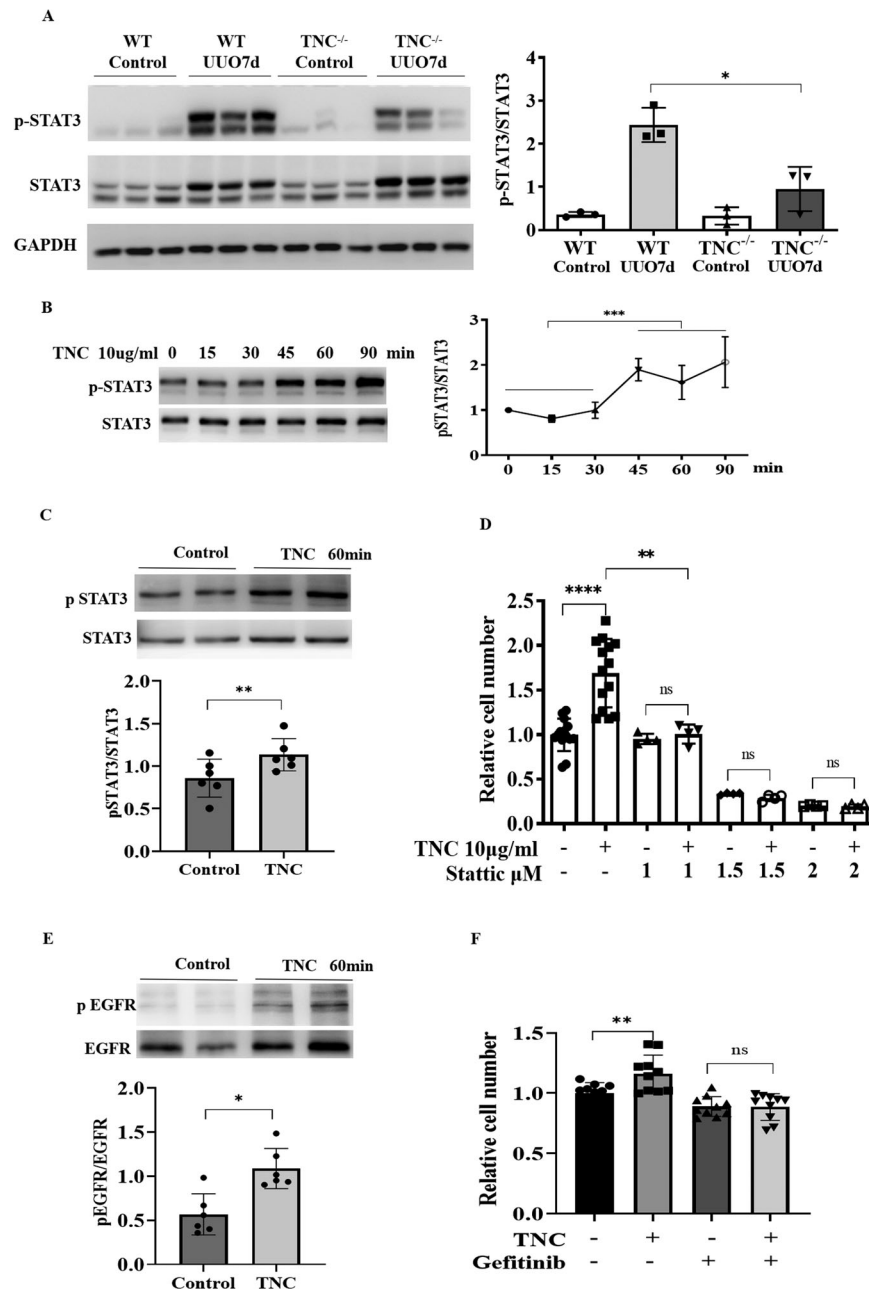


Fig. 5 TNC promoted stromal cells proliferation via STAT3 pathway. In vivo, STAT3 and phospho-STAT3 were markedly increased after UUO, and TNC deletion significantly reduced the phospho-STAT3 levels (A). In cultured fibroblasts, exogenous TNC markedly increased the phosphorylation of STAT3, peaking at 45 min (B, C). The effect of TNC on cell proliferation was blocked by the STAT3 inhibitor Stattic (D). STAT3 is a downstream target of epidermal growth factor receptor (EGFR). TNC also increased the phosphorylation of EGFR (E), and EGFR inhibitor reduced the cell number of TNC-induced fibroblasts proliferation (F).

found that the expanded TNC-expressing cells in the fibrotic renal cortex were not originated from the constitutive TNC-expressing cells in the renal papilla following UUO (Supplementary Fig. 7).

DISCUSSION

Fibrosis is a common event that leads to irreversible loss of organ function and organ failure, and so far has no effective therapy [36]. The excessive deposition of ECM is a key feature of fibrosis. Accumulating evidence has revealed that ECM is not only the product of fibrosis, but also actively drives the persistence of fibrosis [3, 4, 6]. TNC is an ECM glycoprotein that is under tight

temporal and spatial regulation [37, 38]. A recent study suggested that TNC played an important role in kidney fibrosis [18]. Our study showed that (1) the TNC-expression levels and the number of TNC-expressing cells dramatically increased during fibrosis in the kidney; (2) deletion of TNC attenuated kidney fibrosis; (3) TNC facilitated fibrosis, at least in part, by promoting the phosphorylation of STAT3; (4) the cells expressing TNC were mainly localized surrounding the injured tubules, suggesting stromal cells in response to epithelium damage; (5) the cells that produced TNC were a special population of stromal cells, most of which were positive for NG2 and only a few positive for α SMA.

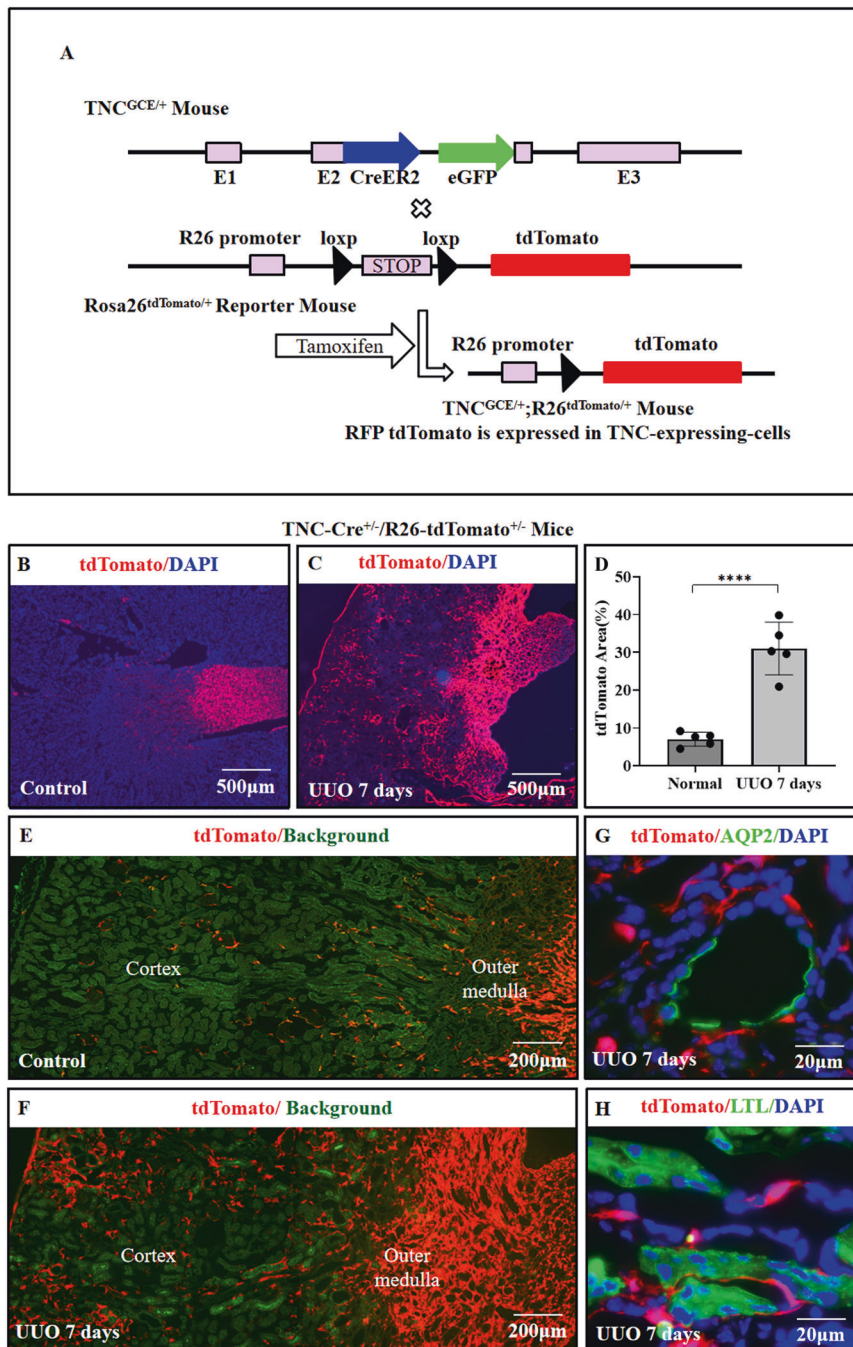


Fig. 6 TNC-expressing cells were significantly increased in fibrotic kidneys. In bi-transgenic TNC^{CreER2-eGFP/+}; R26^{tdTomato/+} mice, the recombination happens in the cells that express TNC in the presence of tamoxifen, and then these TNC-expressing cells and their daughter cells will be labeled with red fluorescence protein tdTomato permanently (A). In normal kidneys, tdTomato also identified TNC-expressing cells rich in the papilla, scattered in the outer medulla, and rare in the cortex (B, E). After UUO (tamoxifen given for 5 days after operation), the tdTomato positive cells were significantly increased in both the renal cortex and medulla (C, D, F, $p < 0.0001$), and these cells were neither AQP2 nor Lotus Tetragnolobus Lectin (LTL) positive tubular epithelial cells (G, H). ($n = 5$, 3 slides for each).

TNC was significantly increased in the kidney with fibrosis induced by UUO or IR injury. Since TNC deficiency significantly increased the severity of acute kidney injury after IR [39], which made the association between TNC and fibrosis more complicated, we investigated the role of TNC in fibrosis and explored the mechanism using UUO model. Our study provided strong evidence that TNC played an important role in promoting kidney fibrosis using a TNC knockout mouse line, consistent with a previous study using siRNA-TNC injection approach [18]. In chronic

kidney disease progression, tubular epithelia have been reported to sense and respond to damage [40–43], followed by interstitial stroma activation [44]. Our study showed that the TNC-expressing cells (eGFP positive cells) in the fibrotic cortex were primarily localized around the injured tubules that had lost their epithelial markers. This specific localization may indicate that TNC plays an important role in linking tubule injury and interstitial cell activation and fibrosis. Interestingly, TNC was reported to be expressed only in the mesenchyme surrounding the epithelia

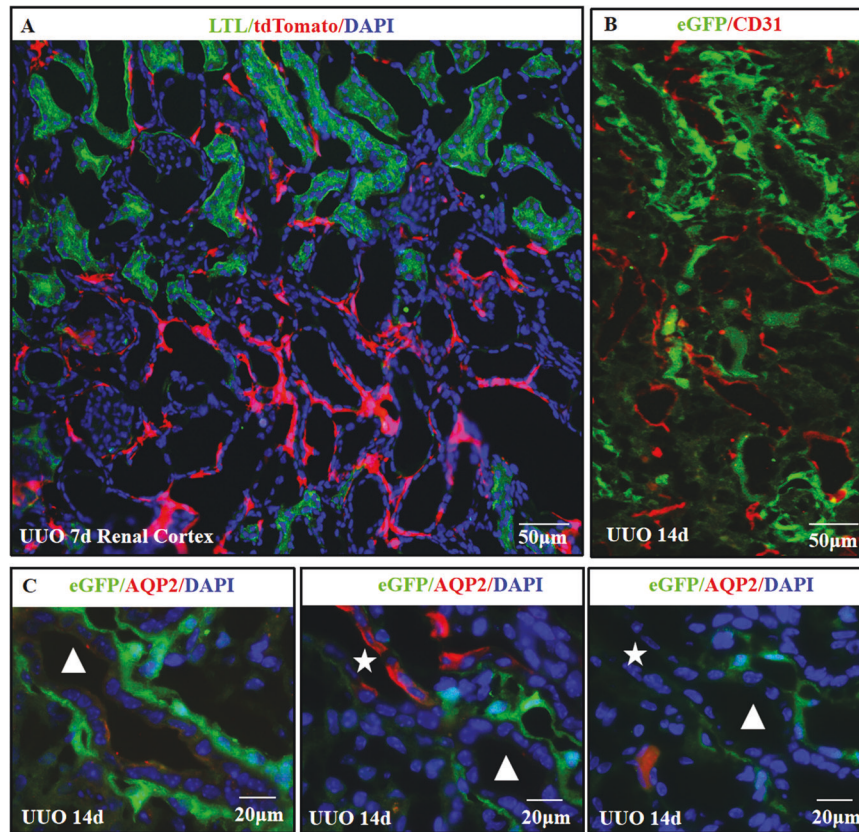


Fig. 7 TNC-expressing cells surrounded the injured renal tubules in fibrotic kidneys. TNC reporter eGFP or tdTomato-positive cells were predominantly located adjacent to the tubular structures in UUO kidneys (A, B). These tubules were negative for CD31, a maker of endothelial cells, suggesting not vessels (B). They were dilated and negative for epithelial markers including LTL and AQP2, presumably injured tubules which lost their markers (A–C). Serial section experiments showed that these tubules (Δ) had continuation to structures with positive AQP2 staining (\star), further supporting that TNC-expressing cells were localized surrounding the injured renal tubules in UUO kidneys (C).

undergoing differentiation during embryonic development [45], and was induced by epithelial-mesenchymal interactions where epithelia were undergoing differentiation or restoration after injury [46]. TGF β , a well-established driver of fibrosis, was found to be upregulated in the injured tubular epithelium [47, 48]. Our study showed that TNC was, at least partially, induced by TGF β (Supplementary Fig. 8). Taken together, these data highlight a potential role of TNC in linking tubule damage to the persistence of interstitial fibrosis.

TNC is a matricellular protein with multiple domains including EGF-like repeats, FNIII repeats and fibrinogen-like globe [13]. These domains can serve as ligands of cell-surface receptors and activate intracellular signals. Receptors for TNC include EGFR, integrins and toll-like receptors [49–52]. These receptors have an enzymatic activity in intracellular domain and usually regulate downstream kinase cascade. Therefore, we screened the kinases and identified STAT3 as a potential signaling pathway mediating the effect of TNC. In UUO-induced kidney fibrosis models, deficiency of TNC gene significantly reduced the phosphorylation of STAT3. In cultured cells, TNC promoted fibroblast proliferation by upregulating the phosphorylation of STAT3, because STAT3 inhibitor blocked the cells proliferation induced by TNC. STAT3 is a transcription factor and has been well demonstrated as a downstream target of EGFR [53, 54]. Although we also found that EGFR inhibition could block the role of TNC on cell proliferation, we did not find that TNC bound with EGFR by co-immunoprecipitation, which may be because the affinity between EGF-like repeats and EGFR is low [49]. Mounting evidence has indicated that STAT3 activation is associated with the proliferation of various cells including

fibroblasts and the development of fibrosis [55–58]. It has been demonstrated that STAT3 promotes cell cycle progression and proliferation by inducing the expression of the target genes, such as cyclin D1 and MYC [59, 60]. STAT3 and its substrates are overexpressed in a wide range of hematopoietic malignancies and solid tumors, and contribute to the proliferative drive [61].

A single nucleus RNA-seq dataset profiling kidney of mouse UUO model at day 14 showed that TNC was predominantly expressed in Act.Fib2 but not Act.Fib1 [20]. Using this dataset, we found that around 60% of Act.Fib2 expressed TNC while less than 5% of Act.Fib1 expressed TNC, and around 6% Act.Fib2 also expressed NG2, PDGFR β and CD44. NG2 is a transmembrane proteoglycan and usually used to label pericytes (NG2⁺PDGFR β ⁺) which had been suggested to be a precursor of myofibroblasts [62]. NG2 expression has also been identified in several types of immature cells (such as progenitor and tumor cells) and is downregulated when cells become mature and quiescent [32, 63, 64]. Similarly, TNC expression has also been found in developing cells, such as progenitors during development, tumor stroma and mesenchymal stem cells [35, 46, 65]. Since co-expression analysis in snRNA-seq might have greatly underestimated the percentage of co-expressing cells due to dropout problem, we co-stained TNC reporter eGFP with these markers and confirmed that most of the TNC-expressing cells were positive for both NG2 and PDGFR β , but not for CD44 (CD 44 is mainly expressed by dedifferentiated or proliferating proximal tubules). Myofibroblasts, characterized by positive staining for α SMA, are the key contributor of kidney fibrosis [66]. It is well known that myofibroblasts are the major source of ECM [67]. Our study showed only some of eGFP-positive

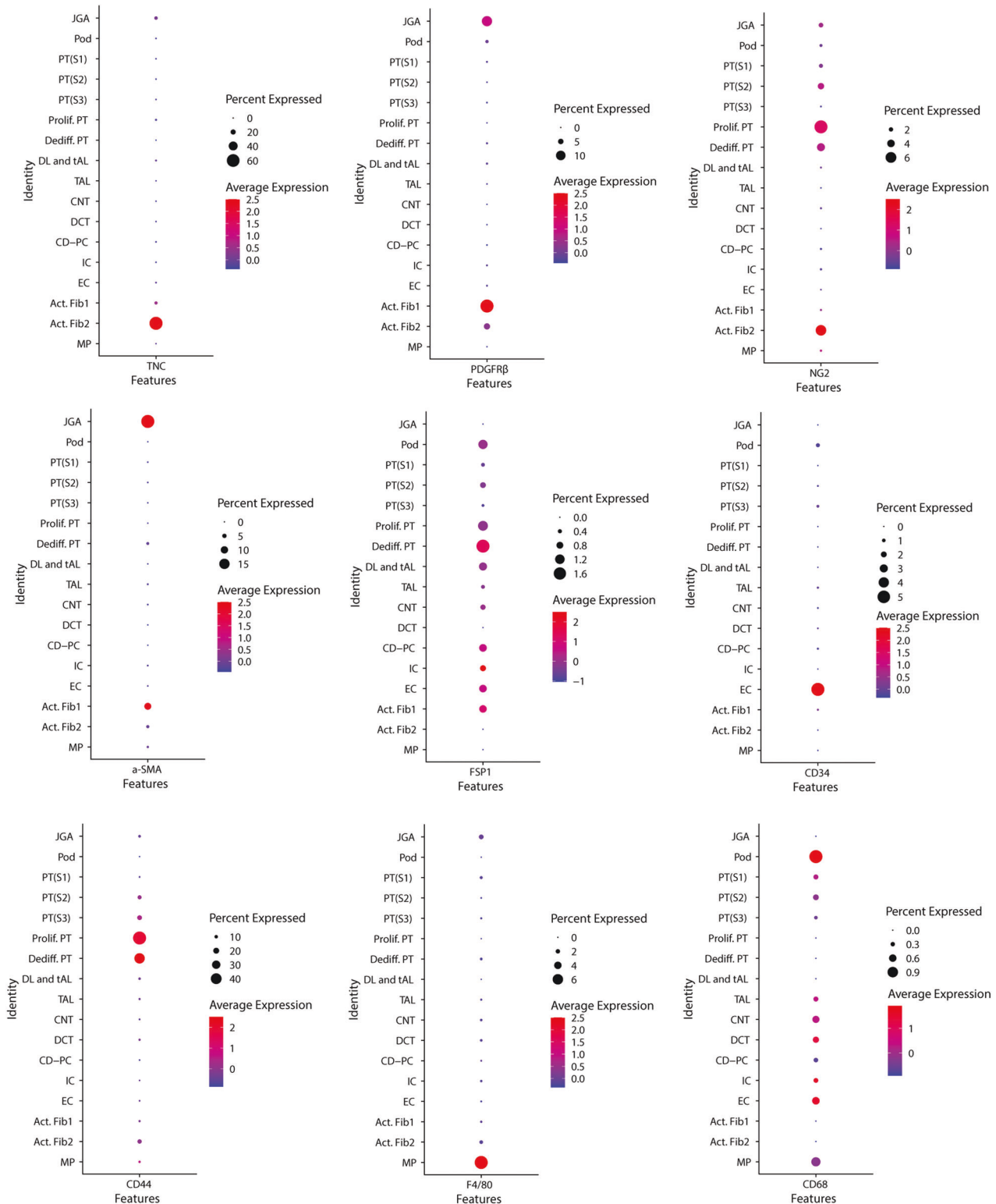


Fig. 8 Single nucleus RNA-seq identified TNC-expressing fibroblasts in mouse UUO kidneys. A previously generated single nucleus RNA-seq dataset profiling kidney of mouse UUO model at day 14 was used for re-analysis. Two subpopulations of activated fibroblasts were identified, with distinct TNC-expression pattern. Around 60% of activated fibroblast 2 (Act.Fib2) expressed TNC, while less than 5% of activated fibroblast 1 expressed TNC. It was observed that around 6% of activated fibroblast 2 expressed PDGFR β , NG2 and CD44. Fibroblasts were almost completely negative in FSP1, CD34, F4/80 and CD68. JGA juxtaglomerular apparatus; Pod podocyte; PT proximal tubule; Prolif proliferating; Dediff dedifferentiated; DL descending limb; tAL thin ascending limb; TAL thick ascending limb; CNT connecting tubule; DCT distal convoluted tubule; CD-PC collecting duct-principal cell; IC intercalated cell; EC endothelial cell; Act activating; Fib fibroblast; MP macrophage.

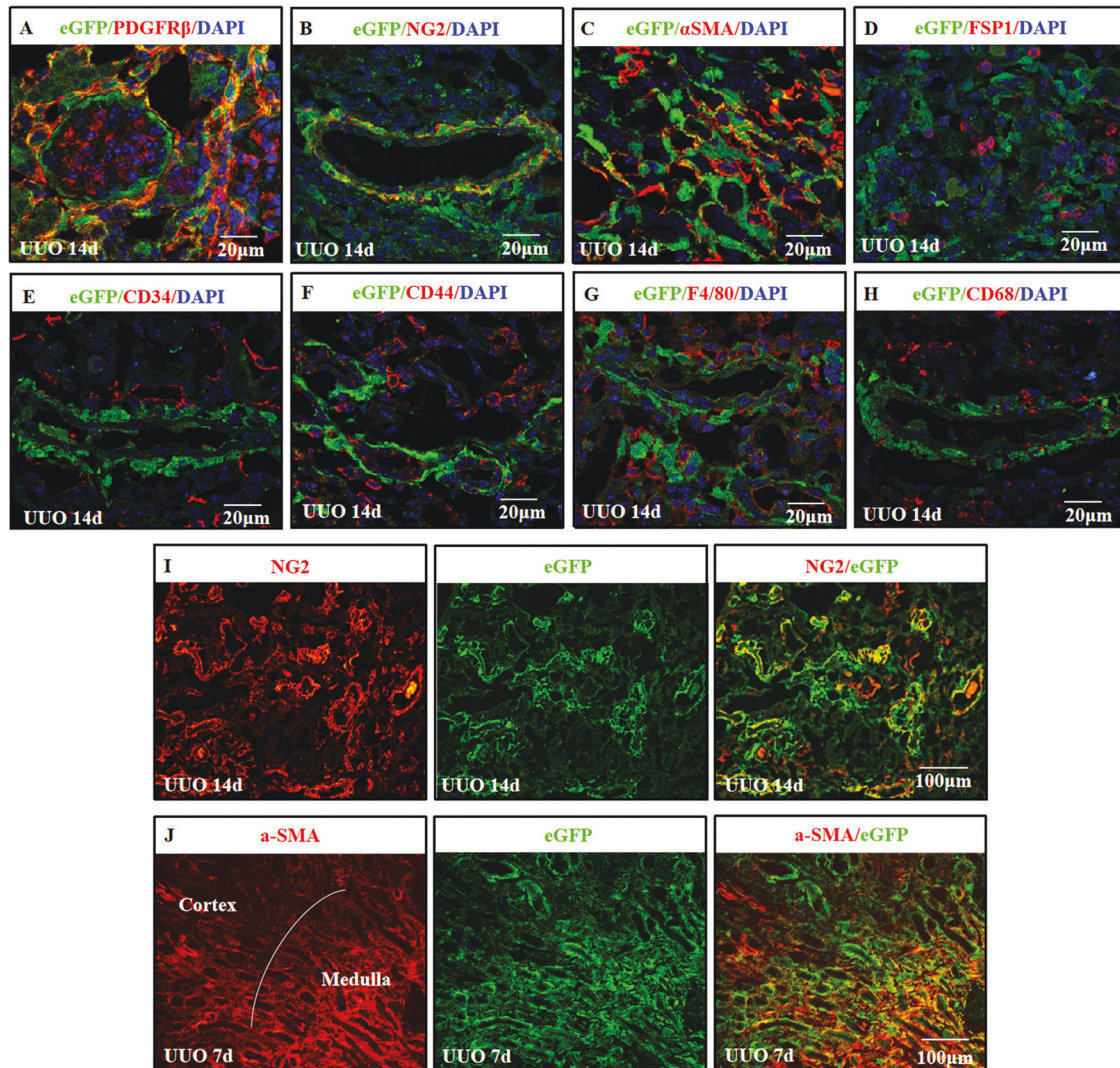


Fig. 9 TNC-expressing cells in fibrotic kidneys were mostly PDGFR β + NG2 + fibroblasts. In TNC^{CreER2-eGFP/+} reporter mice, eGFP positive cells were all PDGFR β positive, consistent with stromal cells (A). Most of the eGFP-positive cells were also NG2 (a marker of pericyte) positive (B, I). Some of eGFP positive cells were α SMA positive, while most of α SMA positive myofibroblasts were not eGFP positive (C, J). These eGFP-positive cells were not positive for FSP1 (D). They were neither CD34 nor CD44 positive progenitors (E, F), and were neither CD68 nor F4/80 positive (G, H). ($n = 4$, 3 sections for each).

cells were α SMA positive, while most of α SMA positive myofibroblasts were not eGFP positive. This result was consistent with the single nucleus RNA-seq analysis, in which α SMA was more expressed by Act.Fib1 rather than Act.Fib2.

It has been reported that renal papilla contains stem cells or progenitors which repopulate after kidney injury [34]. TNC is constitutively expressed in the renal medullary interstitial cells [19]. To examine whether these TNC-expressing cells in renal medulla were progenitors that migrated to renal cortex after injury, we used a genetic mouse model that specifically tracked and fate-mapped renal medullary interstitial TNC-expressing cells. The results demonstrated that the TNC-expressing fibroblasts in renal cortex during fibrosis were not originated from papilla. The origin of TNC-expressing fibroblasts after injury remains unclear and needs further studies.

CONCLUSIONS

In conclusion, our study provides strong evidence that non-structural matrix protein TNC that contains multiple functional domains plays

an important role in kidney fibrosis. TNC is mostly expressed by NG2⁺PDGFR β ⁺ cells around the injured tubules and STAT3 is a signaling pathway at least partially mediating the profibrotic effect of TNC. TNC pathway may serve as a potential therapeutic target to treat interstitial fibrosis and the progression of kidney injury.

DATA AVAILABILITY

Data sharing not applicable to this article as no datasets were generated or analyzed during the current study.

REFERENCES

- Kuncio GS, Neilson EG, Haverty T. Mechanisms of tubulointerstitial fibrosis. *Kidney Int.* 1991;39:550–6.
- Ben Salem C, Slim R, Fathallah N. Fibrosis—a common pathway to organ injury and failure. *N Engl J Med.* 2015;373:95.
- Herrera J, Henke CA, Bitterman PB. Extracellular matrix as a driver of progressive fibrosis. *J Clin Invest.* 2018;128:45–53.
- Wight TN, Potter-Perigo S. The extracellular matrix: an active or passive player in fibrosis? *Am J Physiol-Gastrointest Liver Physiol.* 2011;301:G950–G5.

5. Frangogiannis NG. The extracellular matrix in myocardial injury, repair, and remodeling. *J Clin Invest.* 2017;127:1600–12.
6. Bonnans C, Chou J, Werb Z. Remodelling the extracellular matrix in development and disease. *Nat Rev Mol Cell Biol.* 2014;15:786–801.
7. Clause KC, Barker TH. Extracellular matrix signaling in morphogenesis and repair. *Curr Opin Biotechnol.* 2013;24:830–3.
8. Bornstein P, Sage EH. Matricellular proteins: extracellular modulators of cell function. *Curr Opin Cell Biol.* 2002;14:608–16.
9. Murphy-Ullrich JE, Sage EH. Revisiting the matricellular concept. *Matrix Biol.* 2014;37:1–14.
10. Theocharis AD, Skandalis SS, Gialeli C, Karamanos NK. Extracellular matrix structure. *Adv Drug Deliv Rev.* 2016;97:4–27.
11. Xu Y, Li N, Gao J, Shang D, Zhang M, Mao X, et al. Elevated serum Tenascin-C predicts mortality in critically ill patients with multiple organ dysfunction. *Front Med (Lausanne).* 2021;8:759273.
12. Gao W, Li J, Ni H, Shi H, Qi Z, Zhu S, et al. Tenascin C: a potential biomarker for predicting the severity of coronary atherosclerosis. *J Atheroscler Thromb.* 2019;26:31–8.
13. Midwood KS, Hussenet T, Langlois B, Orend G. Advances in Tenascin-C biology. *Cell Mol Life Sci.* 2011;68:3175–99.
14. De Laporte L, Rice JJ, Tortelli F, Hubbell JA. Tenascin C promiscuously binds growth factors via its fifth fibronectin type III-like domain. *PLoS ONE.* 2013;8:e62076.
15. Shimojo N, Hashizume R, Kanayama K, Hara M, Suzuki Y, Nishioka T, et al. Tenascin-C may accelerate cardiac fibrosis by activating macrophages via the integrin alphaVbeta3/nuclear factor-kappaB/interleukin-6 axis. *Hypertension.* 2015;66:757–66.
16. El-Karef A, Yoshida T, Gabazza EC, Nishioka T, Inada H, Sakakura T, et al. Deficiency of Tenascin-C attenuates liver fibrosis in immune-mediated chronic hepatitis in mice. *J Pathol.* 2007;211:86–94.
17. Bhattacharyya S, Wang W, Morales-Nebreda L, Feng G, Wu M, Zhou X, et al. Tenascin-C drives persistence of organ fibrosis. *Nat Commun.* 2016;7:11703.
18. Fu H, Tian Y, Zhou L, Zhou D, Tan RJ, Stolz DB, et al. Tenascin-C is a major component of the fibrogenic niche in kidney fibrosis. *J Am Soc Nephrol.* 2017;28:785–801.
19. He W, Xie Q, Wang Y, Chen J, Zhao M, Davis LS, et al. Generation of a Tenascin-C-CreER2 knockin mouse line for conditional DNA recombination in renal medullary interstitial cells. *PLoS ONE.* 2013;8:e79839.
20. Wu H, Kirita Y, Donnelly EL, Humphreys BD. Advantages of single-nucleus over single-cell RNA sequencing of adult kidney: rare cell types and novel cell states revealed in fibrosis. *J Am Soc Nephrol.* 2019;30:23–32.
21. Stuart T, Butler A, Hoffman P, Hafemeister C, Papalexi E, Mauck WM 3rd, et al. Comprehensive integration of single-cell data. *Cell.* 2019;177:1888–902 e21.
22. Fushimi K, Uchida S, Hara Y, Hirata Y, Marumo F, Sasaki S. Cloning and expression of apical membrane water channel of rat kidney collecting tubule. *Nature.* 1993;361:549–52.
23. Nielsen S, DiGiovanni SR, Christensen EI, Knepper MA, Harris HW. Cellular and subcellular immunolocalization of vasopressin-regulated water channel in rat kidney. *Proc Natl Acad Sci USA.* 1993;90:11663–7.
24. Heldin CH, Westermark B. Mechanism of action and in vivo role of platelet-derived growth factor. *Physiol Rev.* 1999;79:1283–316.
25. Favaloro EJ, Moraitis N, Koutts J, Exner T, Bradstock KF. Endothelial cells and normal circulating haemopoietic cells share a number of surface antigens. *Thromb Haemost.* 1989;61:217–24.
26. Andrews RG, Singer JW, Bernstein ID. Precursors of colony-forming cells in humans can be distinguished from colony-forming cells by expression of the CD33 and CD34 antigens and light scatter properties. *J Exp Med.* 1989;169:1721–31.
27. Hostettler KE, Gazdhar A, Khan P, Savic S, Tamo L, Lardinois D, et al. Multipotent mesenchymal stem cells in lung fibrosis. *PLoS ONE.* 2017;12:e0181946.
28. Morath I, Hartmann TN, Orian-Rousseau V. CD44: More than a mere stem cell marker. *Int J Biochem Cell Biol.* 2016;81:166–73.
29. Hinz B, Phan SH, Thannickal VJ, Galli A, Bochaton-Piallat ML, Gabbiani G. The myofibroblast: one function, multiple origins. *Am J Pathol.* 2007;170:1807–16.
30. Strutz F, Okada H, Lo CW, Danoff T, Carone RL, Tomaszewski JE, et al. Identification and characterization of a fibroblast marker: FSP1. *J Cell Biol.* 1995;130:393–405.
31. Osterreicher CH, Penz-Osterreicher M, Grivennikov SI, Guma M, Koltsova EK, Datz C, et al. Fibroblast-specific protein 1 identifies an inflammatory subpopulation of macrophages in the liver. *Proc Natl Acad Sci USA.* 2011;108:308–13.
32. Stallcup WB. The NG2 proteoglycan in pericyte biology. *Adv Exp Med Biol.* 2018;1109:5–19.
33. Yan M, Liu S, Zhang M, Lai L, Xie Q, Hao CM. Mesangial cell-derived Tenascin-C contributes to mesangial cell proliferation and matrix protein production in IgA nephropathy. *Nephrology (Carlton).* 2022;27:458–66.
34. Oliver JA, Maarouf O, Cheema FH, Martens TP, Al-Awqati Q. The renal papilla is a niche for adult kidney stem cells. *J Clin Invest.* 2004;114:795–804.
35. Chiquet-Ehrismann R, Orend G, Chiquet M, Tucker RP, Midwood KS. Tenascins in stem cell niches. *Matrix Biol.* 2014;37:112–23.
36. Rockey DC, Bell PD, Hill JA. Fibrosis—a common pathway to organ injury and failure. *N Engl J Med.* 2015;372:1138–49.
37. Jones FS, Jones PL. The tenascin family of ECM glycoproteins: structure, function, and regulation during embryonic development and tissue remodeling. *Dev Dyn.* 2000;218:235–59.
38. Chiquet-Ehrismann R, Chiquet M. Tenascins: regulation and putative functions during pathological stress. *J Pathol.* 2003;200:488–99.
39. Chen S, Fu H, Wu S, Zhu W, Liao J, Hong X, et al. Tenascin-C protects against acute kidney injury by recruiting Wnt ligands. *Kidney Int.* 2019;95:62–74.
40. Kang HM, Ahn SH, Choi P, Ko YA, Han SH, Chinga F, et al. Defective fatty acid oxidation in renal tubular epithelial cells has a key role in kidney fibrosis development. *Nat Med.* 2015;21:37–46.
41. Wu H, Lai CF, Chang-Panesso M, Humphreys BD. Proximal tubule translational profiling during kidney fibrosis reveals proinflammatory and long noncoding RNA expression patterns with sexual dimorphism. *J Am Soc Nephrol.* 2020;31:23–38.
42. Gewin LS. Renal fibrosis: primacy of the proximal tubule. *Matrix Biol.* 2018;68:69:248–62.
43. Qi R, Yang C. Renal tubular epithelial cells: the neglected mediator of tubulointerstitial fibrosis after injury. *Cell Death Dis.* 2018;9:1126.
44. Humphreys BD. Mechanisms of renal fibrosis. *Annu Rev Physiol.* 2018;80:309–26.
45. Aufderheide E, Chiquet-Ehrismann R, Ekblom P. Epithelial-mesenchymal interactions in the developing kidney lead to expression of tenascin in the mesenchyme. *J Cell Biol.* 1987;105:599–608.
46. Midwood KS, Orend G. The role of Tenascin-C in tissue injury and tumorigenesis. *J Cell Commun Signal.* 2009;3:287–310.
47. Meng XM, Nikolic-Paterson DJ, Lan HY. TGF-beta: the master regulator of fibrosis. *Nat Rev Nephrol.* 2016;12:325–38.
48. Yamamoto T, Noble NA, Cohen AH, Nast CC, Hishida A, Gold LI, et al. Expression of transforming growth factor-beta isoforms in human glomerular diseases. *Kidney Int.* 1996;49:461–9.
49. Iyer AK, Tran KT, Borysenko CW, Cascio M, Camacho CJ, Blair HC, et al. Tenascin cytotactin epidermal growth factor-like repeat binds epidermal growth factor receptor with low affinity. *J Cell Physiol.* 2007;211:748–58.
50. Swindle CS, Tran KT, Johnson TD, Banerjee P, Mayes AM, Griffith L, et al. Epidermal growth factor (EGF)-like repeats of human Tenascin-C as ligands for EGF receptor. *J Cell Biol.* 2001;154:459–68.
51. Tucker RP, Chiquet-Ehrismann R. Tenascin-C: Its functions as an integrin ligand. *Int J Biochem Cell Biol.* 2015;65:165–8.
52. Midwood K, Sacre S, Piccinini AM, Inglis J, Trebaul A, Chan E, et al. Tenascin-C is an endogenous activator of Toll-like receptor 4 that is essential for maintaining inflammation in arthritic joint disease. *Nat Med.* 2009;15:774–80.
53. Abdelhamed S, Ogura K, Yokoyama S, Saiki I, Hayakawa Y. AKT-STAT3 pathway as a downstream target of EGFR signaling to regulate PD-L1 expression on NSCLC cells. *J Cancer.* 2016;7:1579–86.
54. Wu J, Patmore DM, Jousma E, Eaves DW, Breving K, Patel AV, et al. EGFR-STAT3 signaling promotes formation of malignant peripheral nerve sheath tumors. *Oncogene.* 2014;33:173–80.
55. Daniel JM, Dutzmann J, Bielenberg W, Widmer-Teske R, Gunduz D, Hamm CW, et al. Inhibition of STAT3 signaling prevents vascular smooth muscle cell proliferation and neointima formation. *Basic Res Cardiol.* 2012;107:261.
56. Seo HY, Jeon JH, Jung YA, Jung GS, Lee EJ, Choi YK, et al. Fyn deficiency attenuates renal fibrosis by inhibition of phospho-STAT3. *Kidney Int.* 2016;90:1285–97.
57. Chakraborty D, Sumova B, Mallano T, Chen CW, Distler A, Bergmann C, et al. Activation of STAT3 integrates common profibrotic pathways to promote fibroblast activation and tissue fibrosis. *Nat Commun.* 2017;8:1130.
58. Ray S, Ju X, Sun H, Finnerty CC, Herndon DN, Brasier AR. The IL-6 trans-signaling-STAT3 pathway mediates ECM and cellular proliferation in fibroblasts from hypertrophic scar. *J Invest Dermatol.* 2013;133:1212–20.
59. Shields BJ, Hauser C, Bukczynska PE, Court NW, Tiganis T. DNA replication stalling attenuates tyrosine kinase signaling to suppress S phase progression. *Cancer Cell.* 2008;14:166–79.
60. Shirogane T, Fukada T, Muller JM, Shima DT, Hibi M, Hirano T. Synergistic roles for Pim-1 and c-Myc in STAT3-mediated cell cycle progression and antiapoptosis. *Immunity.* 1999;11:709–19.
61. Johnson DE, O'Keefe RA, Grandis JR. Targeting the IL-6/JAK/STAT3 signalling axis in cancer. *Nat Rev Clin Oncol.* 2018;15:234–48.
62. Humphreys BD, Lin SL, Kobayashi A, Hudson TE, Nowlin BT, Bonventre JV, et al. Fate tracing reveals the pericyte and not epithelial origin of myofibroblasts in kidney fibrosis. *Am J Pathol.* 2010;176:85–97.
63. Stallcup WB. The NG2 proteoglycan: past insights and future prospects. *J Neurocytol.* 2002;31:423–35.

64. Stallcup WB, Huang FJ. A role for the NG2 proteoglycan in glioma progression. *Cell Adh Migr*. 2008;2:192–201.
65. Chiquet-Ehrismann R, Mackie EJ, Pearson CA, Sakakura T. Tenascin: an extracellular matrix protein involved in tissue interactions during fetal development and oncogenesis. *Cell* 1986;47:131–9.
66. Meran S, Steadman R. Fibroblasts and myofibroblasts in renal fibrosis. *Int J Exp Pathol*. 2011;92:158–67.
67. Klingberg F, Hinz B, White ES. The myofibroblast matrix: implications for tissue repair and fibrosis. *J Pathol*. 2013;229:298–309.

ACKNOWLEDGEMENTS

The authors acknowledge that all authors had access to the data and played a role in writing this article.

AUTHOR CONTRIBUTIONS

Conceptualization, C.M.H., Q.H., M.Z., and X.M.; Methodology, Q.H., C.M.H., X.M., and S.L.; Investigation, Q.H., M.Z., X.M., and S.L.; Writing – Original Draft, C.M.H., Q.H., R.Z. and A.P.; Funding Acquisition, C.M.H., R.Z. and A.P.; Resources, D.S., Y.X., R.C., Y.G., and X.H.

FUNDING

This work was supported by the Natural Science Foundation of China grants NSFC: 81520108006 and 81930120 (C.M.H.), and 82170735 (Q.X.), and 82170750, and VA Merit Awards I01 BX002196 (R.Z.) and I01 BX002025 (A.P.) as well as R01 DK069921 (R.Z.) and R01 DK119212 (A.P.), and P30-DK114809 (A.P. and R.Z.), and 82170750 (X.H.). A.P. is the recipient of a Senior Research Career Scientist award from the Veteran Affairs. The funders had no role in study design, data collection and analysis, decision to publish, or preparation of the manuscript.

COMPETING INTERESTS

The authors declare no competing interests.

ETHICS APPROVAL AND CONSENT TO PARTICIPATE

Human study was approved by the ethics committee of Huashan Hospital, Fudan University, approval number KY2016-394. Informed consent was signed for each patient. Animal study was approved by the Animal Care and Use Committees of Fudan University, approval number 20150588A274.

ADDITIONAL INFORMATION

Supplementary information The online version contains supplementary material available at <https://doi.org/10.1038/s41419-022-05496-z>.

Correspondence and requests for materials should be addressed to Chuan-Ming Hao.

Reprints and permission information is available at <http://www.nature.com/reprints>

Publisher's note Springer Nature remains neutral with regard to jurisdictional claims in published maps and institutional affiliations.



Open Access This article is licensed under a Creative Commons Attribution 4.0 International License, which permits use, sharing, adaptation, distribution and reproduction in any medium or format, as long as you give appropriate credit to the original author(s) and the source, provide a link to the Creative Commons license, and indicate if changes were made. The images or other third party material in this article are included in the article's Creative Commons license, unless indicated otherwise in a credit line to the material. If material is not included in the article's Creative Commons license and your intended use is not permitted by statutory regulation or exceeds the permitted use, you will need to obtain permission directly from the copyright holder. To view a copy of this license, visit <http://creativecommons.org/licenses/by/4.0/>.

© The Author(s) 2022